

Axion–neutrino interactions in seesaw models and astrophysical probes

Polina Kivokurtseva^{a,1}

¹ Institute for Nuclear Research of the Russian Academy of Sciences,
60th October Anniversary Prospect 7a, Moscow 117312, Russia

Received: date / Accepted: date

Abstract We study axion–neutrino interactions in neutrino-mass extensions of the Standard Model, focusing on the Type-I and inverse seesaw. In these frameworks the effective coupling $g_{a\nu}$ is tied to the axion scale and can be constrained using existing astrophysical limits on axion couplings to electrons. We then estimate the impact of axion-mediated scattering on neutrino propagation in two benchmarks: resonant interactions with the $C\nu B$ and scattering on axion dark matter. In the parameter space allowed by current bounds, the resulting optical depths are extremely small, implying no observable signatures with present sensitivities.

Keywords axion, neutrino

1 Introduction

Axions and axion-like particles (ALPs) are hypothetical pseudo-Nambu–Goldstone bosons that arise in a variety of extensions of the Standard Model, most famously in the Peccei–Quinn solution to the strong-CP problem. Beyond their well-known two-photon coupling that enables photon–axion mixing in electromagnetic fields, axions/ALPs can also interact with fermions. In many theoretically well-motivated constructions these couplings scale with the fermion mass, schematically

$$\mathcal{L} \supset i g_{af} a \bar{f} \gamma_5 f, \quad g_{af} \propto \frac{m_f}{f_a}, \quad (1)$$

where a is the axion field, f a Standard Model fermion, and f_a the Peccei–Quinn symmetry-breaking scale (or a generic UV (ultraviolet) scale in ALP scenarios). While the axion–photon interaction has been extensively exploited in laboratory experiments and astrophysical

searches, the axion–lepton sector is currently constrained less tightly and could provide complementary discovery channels.

Of particular interest is the axion–neutrino interaction. Neutrino oscillations demonstrate that neutrinos are massive, implying that an axion–neutrino coupling $g_{a\nu}$ is generically allowed in mass-proportional frameworks.

Several recent works have proposed scenarios that could shed light on axion–neutrino interactions. One example is [1], which probes axion–neutrino couplings in a cosmological context. However, the analysis adopts rather unusual values (several TeV) of the axion decay constant f_a . Such choices of f_a typically imply large $g_{a\gamma\gamma}$ that are already tightly constrained by photon–axion mixing. The cosmological viability of the parameter region discussed in [1] therefore either requires non-standard model-building (e.g., photophobic ALPs or alignment mechanisms that suppress $g_{a\gamma\gamma}$ independently of f_a) or a careful reassessment of existing photon–coupling limits.

On the astrophysical side, Ref. [2] proposed a time-domain search strategy for new neutrino interactions based on propagation-induced delays (“neutrino echoes”) from transient multimessenger sources. This idea provides a clean handle complementary to spectral probes and can be adapted to axion-mediated channels. A related axion–neutrino scenario was explored in Ref. [3], where high-energy neutrino propagation through ultra-light ALP dark matter was studied and the importance of the assumed mass ordering/ flavor structure was emphasized.

In this work we take a complementary approach: rather than postulating an effective $g_{a\nu}$ in isolation, we derive the expected size and structure of the axion–neutrino coupling in minimal neutrino-mass frameworks

^ae-mail: kivokurtseva.pi19@physics.msu.ru

^bINR-TH-2026-004

and relate it to the axion-electron coupling, translating existing bounds on g_{ae} into robust constraints on g_{ν} . We then assess, at the order-of-magnitude level, the discovery prospects in representative astrophysical benchmarks.

The paper is organized as follows. In Sec. 2 we discuss minimal SM extensions that give rise to axion-neutrino interactions. In Sec. 3 we review representative constraints on g_{ae} and translate them into bounds on the neutrino-axion coupling. In Sec. 4 we estimate the optical depths in two illustrative astrophysical scenarios. We briefly discuss our results in Sec. 5.

2 Model overview

In this section we briefly outline how neutrino-axion interactions can emerge in two minimal frameworks: the Type-I seesaw and the inverse seesaw.

Let us consider a theory of neutrino-ALP interactions. As a first step, we consider a minimal extension of the Standard Model that generates neutrino masses through the seesaw mechanism. To account for at least two nondegenerate active-neutrino masses—established by multiple neutrino-oscillation experiments—it is sufficient to introduce at least two right-handed neutrinos N_{iR} ($i = 1, 2$). For simplicity, in our analytic estimates we work with a single right-handed neutrino, denoted N_R . One-generation setup serves as an order-of-magnitude proxy, and the parametric scaling of our results straightforwardly generalizes to the multi-generation case. We also introduce a pseudoscalar axion-like particle (ALP) a , which couples to the neutrino sector through the right-handed neutrinos N_R . In addition, we allow for generic ALP couplings to other SM fields, encoded in \mathcal{L}_{all} ; in particular, a nonzero electron coupling g_{ae} will be used below to translate existing laboratory and stellar limits into constraints on the overall ALP scale and, consequently, on the effective axion-neutrino coupling. The renormalizable Lagrangian then reads

$$\begin{aligned} \mathcal{L} = & \mathcal{L}_{\text{SM}} + i\bar{N}_R \partial N_R - (Y_\nu)_\alpha \bar{L}_\alpha \tilde{H} N_R \\ & - \frac{1}{2} (\mathcal{M}_R) \bar{N}_R^c N_R + \mathcal{L}_{aNN} + \mathcal{L}_{ae} + \text{h.c.} \end{aligned} \quad (2)$$

where $L_\alpha = (\nu_{\alpha L}, \ell_{\alpha L})^\top$ is the SM lepton doublet, $H = (H^+, H^0)^\top$ is the Higgs doublet, $\alpha = e, \mu, \tau$, and $\tilde{H} \equiv i\sigma_2 H^*$. The term \mathcal{L}_{aNN} encodes the ALP-neutrino interaction and may be written as:

$$\mathcal{L}_{aNN} = \frac{C_\nu}{f_a} (\partial_\mu a) \bar{N}_R \gamma^\mu \gamma_5 N_R = -\frac{2iC_\nu}{f_a} m_{N_R} a \bar{N}_R \gamma_5 N_R, \quad (3)$$

Analogously, for the electron interaction we obtain:

$$\mathcal{L}_{ae} = -\frac{2iC_e}{f_a} m_e a \bar{e} \gamma_5 e, \quad (4)$$

After the electroweak symmetry breaking (EWSB), the neutral-fermion mass matrix in the (ν_L, N_R^c) basis takes the form

$$\mathcal{M}_\nu = \begin{pmatrix} 0 & \mathcal{M}_D \\ \mathcal{M}_D^\top & \mathcal{M}_R \end{pmatrix}, \quad (5)$$

where $\mathcal{M}_D = Y_\nu v / \sqrt{2}$ is the Dirac mass matrix and \mathcal{M}_R is the Majorana mass matrix of the right-handed neutrino(s). Diagonalizing with a unitary matrix U ,

$$U^\dagger \mathcal{M}_\nu U^* = \begin{pmatrix} m_\nu & 0 \\ 0 & M_R \end{pmatrix}, \quad (6)$$

where m_ν and M_R are diagonal mass matrices.

In the seesaw limit $|\mathcal{M}_D| \ll |\mathcal{M}_R|$ the active-sterile mixing is controlled by

$$\Theta \equiv \mathcal{M}_D \mathcal{M}_R^{-1}, \quad (7)$$

so that the full diagonalization matrix can be written in a 2×2 block form,

$$U = \begin{pmatrix} U_{\nu\nu} & U_{\nu N} \\ U_{N\nu} & U_{NN} \end{pmatrix}, \quad U_{N\nu} \simeq \Theta, \quad U_{\nu\nu} \simeq \mathbf{1} + \mathcal{O}(\Theta^2). \quad (8)$$

We will consistently retain only the leading terms in Θ , implying $|U_{\nu\nu}|^2 = \mathcal{O}(1)$ while $|U_{\nu N}|^2 \simeq |U_{N\nu}|^2 = \mathcal{O}(\Theta^2)$. For the partial widths of the relevant two-body decays we get:

$$\Gamma(a \rightarrow \nu\nu) = \frac{m_N^2 m_a |U_{\nu N}|^4}{2\pi f_a^2} \sqrt{1 - \frac{4m_\nu^2}{m_a^2}} \quad (9)$$

Integrating out the heavy state leads to an effective interaction for the light neutrinos. At leading order in Θ , this EFT (effective field theory) reproduces the same $a \rightarrow \nu\nu$ amplitude as the full theory, up to higher-order corrections in Θ .

A similar result is obtained if we instead employ the inverse seesaw mechanism for mass generation. Compared to the Type-I seesaw, the inverse seesaw (ISS) introduces an additional set of SM-singlet neutral fermion S_R . The neutral-lepton field content is therefore (ν_L, N_R, S_R) . After electroweak symmetry breaking, the mass Lagrangian reads

$$\mathcal{L}_{\text{mass}} = -\bar{N}_R m_D \nu_L - \bar{S}_R M N_R^c - \frac{1}{2} \bar{S}_R \mu S_R^c + \text{h.c.}, \quad (10)$$

where m_D is a Dirac mass matrix generated by Yukawa couplings to the Higgs field, M is a Dirac mass term

linking N_R and S_R , and μ is a small Majorana mass term for S_R that softly breaks lepton number.

In the basis (ν_L, N_R^c, S_R^c) the (symmetric) neutrino mass matrix is

$$\mathcal{M}_\nu = \begin{pmatrix} 0 & m_D^\top & 0 \\ m_D & 0 & M^\top \\ 0 & M & \mu \end{pmatrix}. \quad (11)$$

For $|\mu| \ll |M|$ and $|m_D| \sim |M|$, the matrix can be diagonalized perturbatively. Denoting by O the orthogonal matrix that diagonalizes \mathcal{M}_ν ,

$$O^\top \mathcal{M}_\nu O = \text{diag}(m_\nu, m_+, m_-), \quad (12)$$

with approximate eigenvalues

$$m_\nu \simeq \mu \frac{m_D^2}{M^2}, \quad (13)$$

$$m_\pm \simeq \pm \sqrt{M^2 + m_D^2} + \mu \frac{M^2}{2(M^2 + m_D^2)}. \quad (14)$$

In our notation we need to look at axion interaction with ν , S and N_R , we can write it for $\psi = (\nu, N, S)^T$:

$$\mathcal{L}_{a\psi\psi} = \frac{1}{f_a} (\partial_\mu a) \bar{\psi} \gamma^\mu \gamma_5 Q \psi = \frac{1}{f_a} (\partial_\mu a) \bar{\nu} \gamma^\mu \gamma_5 G \nu, \quad (15)$$

where $Q = \text{diag}(c_\nu, c_N, c_S)$ and $G = O^T Q O$. We can rewrite it the following way:

$$\mathcal{L}_{a\psi\psi} = -i \frac{a}{f_a} \sum_{i,j} (m_i + m_j) G_{ij} \bar{\nu}_i \gamma_5 \nu_j, \quad (16)$$

We translate the constraints on the axion-electron coupling g_{ae} into constraints on the axion decay constant f_a . This, in turn, allows us to infer the corresponding bounds on the neutrino-axion coupling.

$$g_{a\nu} = g_{aee} \frac{C_\nu m_\nu}{C_e m_e} \quad (17)$$

Here C_ν is the dimensionless PQ charge of the heavy right-handed neutrino N_R and C_e is the analogous coefficient for the electron. The effective coupling of the ALP to the light neutrino mass eigenstate is generated through active-sterile mixing upon integrating out N_R .

In the inverse seesaw the smallness of m_ν is controlled by the lepton-number-violating parameter μ rather than by Θ [4]. $C_\nu/C_e \sim \mathcal{O}(1)$ then gives a direct estimate of $g_{a\nu}$. In the Type-I seesaw, by contrast, $|\Theta|^2 = m_\nu/M_R \ll 1$, and the same equation provides a conservative upper bound on $g_{a\nu}$, saturated in the inverse-seesaw regime. Since the optical depths computed in Sec. 4 are far below unity already at this upper bound, our conclusions hold for the Type-I case.

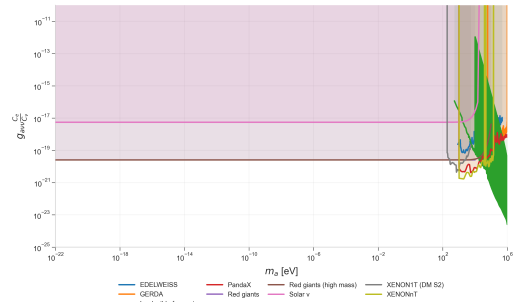


Fig. 1 Constraints on the axion-electron coupling g_{ae} and the corresponding inferred bounds on the neutrino-axion coupling $g_{a\nu}$ obtained via Eq. (17). The mass of neutrino is taken $m_\nu = 0, 1\text{eV}$

3 Present constraints

There exist several constraints on the axion-electron coupling g_{ae} .

Direct-detection experiments have provided important laboratory constraints on ALPs. XENON100 was among the first detectors to set limits on ALP interactions [5]. Subsequent results were obtained (or projected) by experiments such as DARWIN [6], EDELWEISS [7], and GERDA [8].

Astrophysical considerations yield some of the most stringent bounds. In particular, the evolution of red-giant-branch stars constrains g_{ae} [9]. Additional limits arise from solar physics, including searches based on solar axions and solar-neutrino measurements [10].

Additional cosmological constraints could be included; however, in this work we focus only on bounds relevant for ALPs and do not assume a particular role of the ALP in cosmology.

Using Eq. (17), we obtain the corresponding constraints on the neutrino-axion coupling, shown in Fig. 1.

4 Astrophysical scenarios

The axion-neutrino interaction is expected to be extremely weak; nevertheless, it may be probed in environments characterized by high particle densities. We consider two scenarios in which the neutrino-axion interaction could potentially be tested. In the first scenario we explore the resonant interactions with the $C\nu B$. For the second scenario we test scattering on axion dark matter.

4.1 Time delay

Our first scenario follows Ref. [2] and is based on a time-delay signal induced by neutrino scattering during propagation from a transient source. In particular,

we consider scattering of high-energy neutrinos on $C\nu B$ neutrinos along the line of sight ($\nu\nu \rightarrow a \rightarrow \nu\nu$). In the absence of a direct measurement of the cosmic neutrino background, we adopt the standard Λ CDM prediction for the relic neutrino distribution. For our order-of-magnitude estimates we treat the $C\nu B$ number density as homogeneous and time-independent along the line of sight, using the present-day mean value $n \approx 56 \text{ cm}^{-3}$ per species. In our estimate we take the cosmic neutrinos to be at rest. Assuming that the process is resonant, with $s \simeq 2m_\nu \epsilon_\nu$, where ϵ_ν is energy of initial neutrino, the scattering cross section can be written as

$$\frac{d\sigma_{\nu\nu}}{d\cos\theta} = \frac{g_{a\nu}^4}{32m_\nu^2\pi} \frac{s^2}{(s - m_a^2)^2 + m_a^2\Gamma^2} \times \left(1 + \frac{\epsilon_\nu}{m_\nu}(1 - \cos\theta)\right)^{-2}, \quad (18)$$

where $\Gamma = \Gamma_{a\gamma\gamma} + \Gamma_{a\nu\nu}$. To estimate the impact of this process, we compute the optical depth $\tau = n\sigma_{\nu\nu}D$, where D is a distance from the source. As a benchmark source we take SN 1987A [11]. We use the largest currently allowed value of $g_{a\nu}$ from Fig. 1 and set the neutrino mass to $m_\nu = 0,1\text{eV}$. The probability for a neutrino to scatter on a $C\nu B$ neutrino along the line of sight is $1 - e^{-\tau}$. The optical depth can be estimated as $\tau \approx 10^{-53}$. Hence the overwhelming majority of neutrinos propagate without interacting.

In order to assess whether the effect can become significant, we next consider a second scenario in which the ALP constitutes cold dark matter. In this case the relevant target density is $n_a = \rho_{\text{DM}}/m_a$, which is enhanced for smaller ALP masses. Therefore, we focus on an ultralight ALP. We now turn to a more detailed discussion of this scenario.

4.2 Axion flux

Our second scenario is based on neutrino interactions with axion dark matter. A similar scenario was discussed in [3], illustrating the crucial role of the axion dark-matter density. As a baseline value we take the local Milky Way dark-matter density $\rho_{\text{DM}} = 0.4 \text{ GeV/cm}^3$ [12], assuming that all of the dark matter is composed of axions.

Assuming $\epsilon_\nu \gg m_\nu$ and $m_a \ll m_\nu$, the neutrino-ALP scattering cross section can be approximated as [3]

$$\sigma_{\nu a} \simeq \frac{g_{a\nu}^4}{16\pi\epsilon_\nu(m_a + 2\epsilon_\nu)} \left[2\ln\left(\frac{\epsilon_\nu}{m_\nu}\right) - 7\right].$$

We emphasize that n_a is highly sensitive to the ALP mass: for ultralight m_a the number density becomes

very large, which maximizes the interaction probability at fixed (ρ_{DM}). In this scenario we get $\tau \approx 10^{-15}$. Even though the optical depth in this scenario is significantly larger than in the first scenario, it should be noted that, for ultralight dark matter the axion behaves as a classical field rather than as individual particles [13].

5 Discussion

Neither of the two scenarios discussed above yields an observable probe of the axion-neutrino interaction with current sensitivities. We also explored several other scenarios, including scattering on relic neutrinos into three neutrinos via the Fermi interaction, as well as channels involving a neutrino and a photon; in all cases the predicted effects remain unobservable.

Our estimates depend on astrophysical and cosmological assumptions. For the time-delay scenario, the $C\nu B$ is taken to be homogeneous with a standard Λ CDM number density; local clustering of relic neutrinos could in principle enhance the effect, but would need to be extremely large to change our qualitative conclusion. For the axion-dark-matter scenario, the result scales with the assumed dark-matter profile and local density; varying ρ_{DM} within commonly used ranges changes τ only by an overall factor 1 and does not overcome the suppression by many orders of magnitude found above.

A further approximation concerns the ultralight axion limit. When m_a is sufficiently small, the axion dark matter is more appropriately described as a coherent classical field rather than a gas of individual particles. In that regime, the relevant observable may be a oscillation effect induced by a background rather than rare hard scattering events, and the particle-scattering picture used here should be regarded as a conservative order-of-magnitude estimate.

From the perspective of discovery potential, the most promising directions are environments with substantially enhanced target densities like dense dark-matter regions.

It is possible to decouple the value of $g_{a\gamma\gamma}$ from f_a through the higher-order theories (see e.g. [14]). It can be done so f_a will take a lower value and make axion-neutrino interaction stronger. We will leave it for future studies.

6 Conclusions

In this paper we studied axion-neutrino interactions in minimal extensions of the Standard Model that generate neutrino masses, focusing on the Type-I seesaw

and the inverse seesaw. We then considered astrophysical scenarios in which such interactions could leave an observable effect.

More broadly, in realistic realizations of these neutrino-mass mechanisms the size of the axion-neutrino coupling is not a freely adjustable parameter: it is tied to the same axion scale and charge assignments that also control the ALP couplings to charged leptons. As a result, astrophysical limits on the axion-lepton sector translate into a stringent upper bound on $g_{a\nu}$, which suppresses any neutrino-propagation signature in the environments considered here. Therefore, within minimal and phenomenologically viable Type-I and inverse-seesaw models, none of our benchmark scenarios can yield an observable effect; detectable signals would require either non-minimal model-building that decouples $g_{a\nu}$ from charged-lepton constraints and astrophysical settings with drastically enhanced effective target densities.

Acknowledgements The author is very grateful to Sergey Troitsky, Dmitry Kalashnikov, Dmitry S. Gorbunov for useful discussions. This work is supported by the Russian Science Foundation, grant 22-12-00253-P.

References

1. F.F. Deppisch, T.E. Gonzalo, C. Majumdar, Z. Zhang, *Journal of Cosmology and Astroparticle Physics* **2025**(02), 054 (2025). DOI 10.1088/1475-7516/2025/02/054. URL <http://dx.doi.org/10.1088/1475-7516/2025/02/054>
2. K. Murase, I.M. Shoemaker, *Phys. Rev. Lett.* **123**(24), 241102 (2019). DOI 10.1103/PhysRevLett.123.241102
3. M.M. Reynoso, O.A. Sampayo, A.M. Carulli, *The European Physical Journal C* **82**(3) (2022). DOI 10.1140/epjc/s10052-022-10228-w. URL <http://dx.doi.org/10.1140/epjc/s10052-022-10228-w>
4. R.N. Mohapatra, J.W.F. Valle, *Phys. Rev. D* **34**, 1642 (1986). DOI 10.1103/PhysRevD.34.1642. URL <https://link.aps.org/doi/10.1103/PhysRevD.34.1642>
5. Aprile, E., et al., *Physical Review D* **90**(6) (2014). DOI 10.1103/physrevd.90.062009. URL <http://dx.doi.org/10.1103/PhysRevD.90.062009>
6. Aalbers, J., et al., *Journal of Cosmology and Astroparticle Physics* **2016**(11), 017–017 (2016). DOI 10.1088/1475-7516/2016/11/017. URL <http://dx.doi.org/10.1088/1475-7516/2016/11/017>
7. Armengaud, E., et al., *Physical Review D* **98**(8) (2018). DOI 10.1103/physrevd.98.082004. URL <http://dx.doi.org/10.1103/PhysRevD.98.082004>
8. Agostini, M., et al., *Physical Review Letters* **125**(1) (2020). DOI 10.1103/physrevlett.125.011801. URL <http://dx.doi.org/10.1103/PhysRevLett.125.011801>
9. F. Capozzi, G. Raffelt, *Physical Review D* **102**(8) (2020). DOI 10.1103/physrevd.102.083007. URL <http://dx.doi.org/10.1103/PhysRevD.102.083007>
10. P. Gondolo, G.G. Raffelt, *Physical Review D* **79**(10) (2009). DOI 10.1103/physrevd.79.107301. URL <http://dx.doi.org/10.1103/PhysRevD.79.107301>
11. H. Yüksel, J.F. Beacom, *Physical Review D* **76**(8) (2007). DOI 10.1103/physrevd.76.083007. URL <http://dx.doi.org/10.1103/PhysRevD.76.083007>
12. Weber, M., de Boer, W., *A&A* **509**, A25 (2010). DOI 10.1051/0004-6361/200913381. URL <https://doi.org/10.1051/0004-6361/200913381>
13. A. Berlin, *Physical Review Letters* **117**(23) (2016). DOI 10.1103/physrevlett.117.231801. URL <http://dx.doi.org/10.1103/PhysRevLett.117.231801>
14. V.A. Rubakov, *Journal of Experimental and Theoretical Physics Letters* **65**(8), 621–624 (1997). DOI 10.1134/1.567390. URL <http://dx.doi.org/10.1134/1.567390>